BMC Medical Imaging

RESEARCH

Open Access

Lymphatic plastic bronchitis: a study based on CT and MR lymphangiography

Qi Hao[1], Yan Zhang[3], Xingpeng Li[2], Xiaoli Sun[2], Nan Hong[1*] and Rengui Wang[2*]

Abstract

Objectives To investigate the diagnostic value of CT lymphangiography (CTL) and non-contrast MR lymphangiography (MRL) in lymphatic plastic bronchitis.

Materials and methods The clinical and imaging data of 31 patients with lymphatic plastic bronchitis diagnosed by clinical, imaging and pathological results were retrospectively analyzed. All patients underwent CTL and MRL. The imaging findings of patients include: (i) abnormal lymphatic reflux of the bronchial mediastinal trunk, the subclavian trunk, the cervical trunk, the thoracic duct and the right lymphatic duct; Abnormal CTL reflux refers to abnormal iodide deposition outside the normal lymphatic reflux pathway; If the MRL can observe abnormal lymphatic dilatation, hyperplasia, or morphological abnormalities, it is assumed that abnormal lymphatic reflux may be present.; (ii) abnormal morphological changes of lymphatic vessels at the extremity of the thoracic duct, the extremity of the right lymphatic duct and the mediastinum, such as spot-like or tubular, cystic changes; (iii) abnormal CTL and MRL signs in the lungs. The Mcnemar test was used to compare the parameters between CTL and MRL. $P<0.05$ was statistically significant. The Kappa test was used to evaluate the consistency of CTL and MRL in evaluating lymphatic plastic bronchitis.

Results MRL was superior to CTL in detecting abnormal lymphatic reflux in the right lymphatic vessel, thoracic duct, cervical trunk and subclavian trunk ($P<0.05$).and the diagnostic consistency was general (Kappa < 0.40). There was no significant difference between MRL and CTL in the detection of abnormal lymphatic reflux in the bronchial mediastinal trunk ($P>0.05$), and the diagnostic consistency was good (Kappa > 0.60). MRL was superior to CTL in detecting lymphatic abnormalities such as cystic changes at the extremity of the thoracic duct, spot-like or tubular changes at the extremity of the right lymphatic duct, cystic changes at the extremity of the right lymphatic duct, and cystic changes in the mediastinum ($P<0.05$), and the diagnostic consistency was poor, fair, fair, and moderate (Kappa < 0.60), respectively. MRL and CTL showed abnormal signs in the lung: CTL was superior to MRL in showing the thickening of interlobular septum, lung nodules and airway stenosis ($P<0.05$), and the diagnostic consistency was moderate, moderate and poor (Kappa < 0.60). There was no significant difference between CTL and MRL in atelectasis, consolidation in lobar and segmental distribution, consolidation in non-lobar and segmental distribution, and the thickening of the bronchovascular bundle ($P>0.05$), and the diagnostic consistency was very good, very good, good, good (Kappa > 0.60). There was no significant difference between CTL and MRL in ground glass opacity, airway wall thickening and intralobular interstitial thickening ($P>0.05$), and the diagnostic consistency was average, fair and poor (Kappa < 0.40).

*Correspondence:
Nan Hong
hongnan@bjmu.edu.cn
Rengui Wang
wangrg@bjsjth.cn
Full list of author information is available at the end of the article

Conclusion The MRL is superior to CTL in showing the abnormalities of the thoracic duct, the right lymphatic duct and other abnormal lymphatic vessels. CTL is superior to MRL in the detection of pulmonary abnormalities. The combination of CTL and MRL can provide more comprehensive imaging information for diagnosing and treating lymphatic plastic bronchitis.

Keywords Lymphatic, Plastic bronchitis, Lymphangiography, Tomography, X-ray, Magnetic resonance imaging

Introduction

Lymphatic plastic bronchitis (PB) is a rare lung disease. It is named after the abnormal lymph flow caused by various causes, leading to the abnormal accumulation of lymph in the bronchus and the formation of tree-like substances, the incidence and gender preference of this disease are not clear. This disease is often accompanied by local or widespread bronchial obstruction or varying degrees of respiratory dysfunction, leading to severe and life-threatening respiratory distress [1]. According to the source of cast substance production, PB can be divided into lymphatic and non-lymphatic [2]. The former is the formation of airway chylous leakage caused by abnormal lymphatic reflux, which is relatively rare and mostly reported as case reports [3, 4]. Unenhanced magnetic resonance lymphangiography (MRL) uses heavily T2-weighted images to identify slow-flowing lymph [5], which is safe, non-invasive, and does not need any contrast agent. It can display the whole picture of lymphatic vessels and help identify abnormal changes in them. However, MRL images are easily disturbed by artifacts, and the thoracic duct may be poorly displayed [6–8]. Besides, abnormal signs in the lung were poorly displayed in MRL [9]. Computed tomography lymphangiography (CTL) shows the abnormal lipiodol deposition on CT scans after direct lymphangiography(DLG), suggesting the abnormalities of corresponding lymphatic vessels. CTL has an important reference value for the diagnosis and evaluation of lymphatic lesions [10, 11]. CTL has high-density resolution and powerful post-processing capabilities, but it has ionizing radiation. The CTL and MRL manifestations of lymphatic PB have been reported in the literature [4, 12]. However, the comparative study of CTL and MRL for this disease has not been reported. Therefore, the study aimed to explore the application value of MRL and CTL in diagnosing lymphatic PB.

Materials and methods

Patients

Between January 2013 and December 2021, the clinical and imaging data of 36 patients diagnosed with lymphatic PB were retrospectively reviewed at Beijing Shijitan Hospital, Capital Medical University. Diagnostic criteria: lymphatic PB is associated with primary lymphatic vessel dysplasia and coughs up bronchial tree tube type substance, which is confirmed as lymphatic PB by the above criteria. The inclusion and exclusion criteria are shown in Fig. 1. Patients were selected for the study if they met

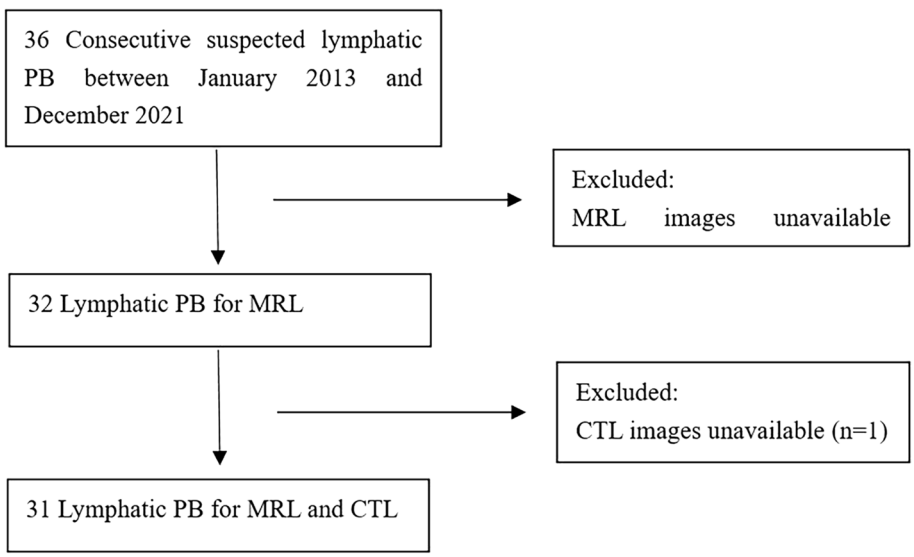

Fig. 1 Flow diagram of study cohort

the following criteria: (i) cough up or pick up the bronchial tree-like substances with bronchoscopy; (ii) CTL and MRL were performed, and the abnormalities of lymphatic vessels. The exclusion criteria were patients who did not undergo CT examination after direct lymphangiography and patients who did not undergo MRL. Page 4, lines 86–88. Among the 36 patients, 4 patients did not undergo MRL, and 1 patient did not undergo CTL. Finally, 31 patients were enrolled in this study, including 17 males and 14 females. The age at diagnosis ranged from 1 to 65 years, with a median age of 39 years, and the duration of the disease ranged from 2 months to 40 years. The clinical symptoms included cough (31 cases), expectoration ($n=31$), chest tightness ($n=18$), fever ($n=6$) and hemoptysis ($n=4$). There was chylous pericardial effusion ($n=5$), chylous pleural effusion ($n=11$), chylous ascites ($n=1$), bone lymphangioma ($n=5$) and spleen lymphangioma ($n=5$).

In our study, 30 of 31 patients underwent the thoracic duct outlet surgery. 24 patients underwent CTL before the thoracic duct outlet surgery and chest CT scan between 4 and 19 days after the surgery. Among them, lung lesions were alleviated in 16 patients. No significant changes were found in 3 patients. The lung lesions were aggravated in 5 patients.

Computed tomography ang magnetic resonance lymphangiography

CTL: The DLG was performed using a GE Innova 2000-IQ DSA machine (AXIOM; Siemens Healthineers, Erlangen, Germany). The skin incision and subcutaneous lymphatic puncture were performed between the 1st and 2nd and 2nd and 3rd toes of the healthy or less edematous side of the foot. 8 ~ 20 ml of ultra-liquid lipiodol (Lipiodol UF Guerbet, France) was injected through a high-pressure syringe at a rate of 1 ~ 2 ml per minute. The reflux of lipiodol along lymphatic vessels was dynamically observed under lymphangiography. Chest, abdomen and pelvis multi-slice spiral CT scan was performed 20 min to 2 h after DLG. The CT equipment was a Siemens 16-slice CT machine or a Philips 256-slice iCT machine. The CT scan ranged from the level of the inferior border of the thyroid cartilage in the neck to the inferior border of the pubic symphysis. The scan parameters were set as follows: tube voltage of 80–120 kV, tube current of 250–300 mA, slice thickness of 5 mm and pitch of 1. After scanning, the raw data were transferred to the CT workstation for postprocessing reconstruction, such as multiplanar reformation (MPR), maximum intensity projection (MIP), and volume rendering (VR).

MRL: Philips Ingenia 3.0 T MR Scanner, head coil combined with body coil, 3D heavy T2-weighted water imaging sequence was used for MRL. Parameters: TR 2500–3000 ms, TE 550–600 ms, echo chain length 85–105, scanning range 36 cm × 30 cm × 9 cm, voxel 10 mm × 10 mm × 10 mm. The number of acquisition layers was 90, and the scanning range covered the root of the neck to the level of the pelvic floor. Images were acquired using a 100 ms breath-gated end-expiration delay. After scanning, the raw data were sent to the workstation, and MRL images were obtained after projection reconstruction with maximum signal intensity.

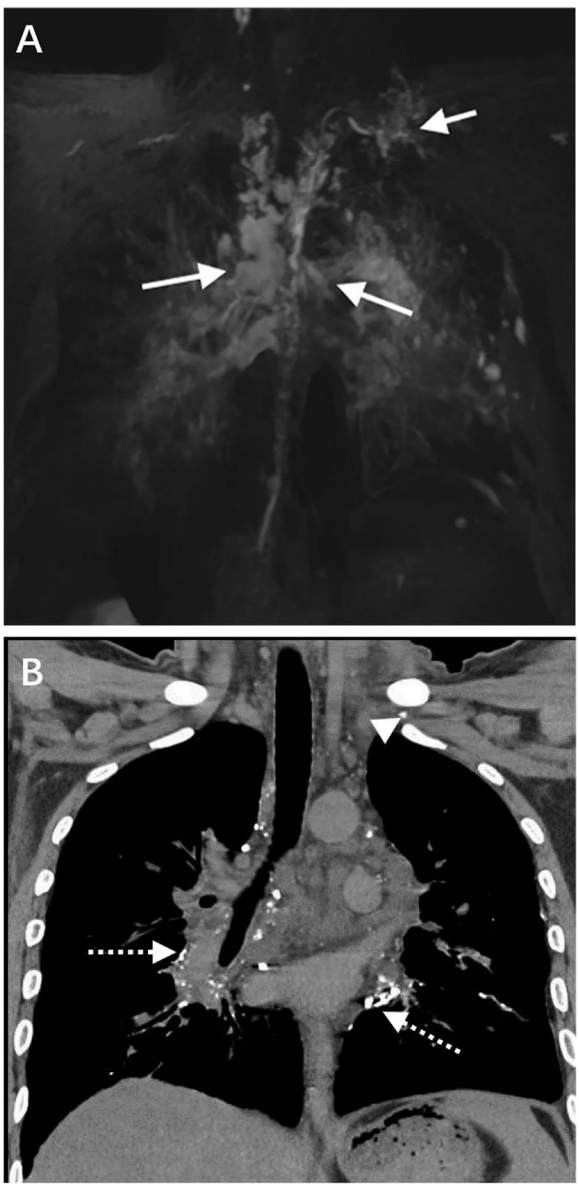

Fig. 2 **A** The coronal MRL shows cystic and tortuous lymphatic vessels in the extremity of thoracic duct *(white short arrow)* and bilateral hilum *(white long arrow)*. **B** The coronal CTL shows abnormal contrast medium accumulation in the bilateral hilum *(white long dashed arrow)* and subclavian region *(white arrowhead)*

Imaging analysis

The quality of the MRL and CTL images met the criteria for disease assessment. All images were reviewed by two radiologists using a double-blind method (Zhang- Y and Li-X, a diagnostic radiologist with over 5 years of experience). The two consulted and reached a consensus when the observations were inconsistent.

Images were classified as follows.

CTL: (i) Abnormal lymphatic reflux: When lipiodol is injected into the superficial lymphatic vessels of the foot, lipiodol will flow into the thoracic duct along the ipsilateral iliac lymphatic vessels, lumbar trunk, and cisterna chyli. Therefore, abnormal lymphatic reflux was defined as the distribution of lipiodol in clumps, tortuous, or strips at any other site. (ii) Abnormal morphology of lymphatic vessels: spot-like or tubular hypodensity, cystic hypodensity. (iii) Abnormal signs of the lungs: ① Parenchymal changes of the lungs: a. ground glass opacity (GGO): GGO can be divided into parenchymal and interstitial GGO. The former refers to the diffuse GGO with central distribution caused by airway inhalation, which can be divided into acinar GGO (mostly confined to a lobular segment, about 5–10 mm in diameter, blurred margin) and ordinary GGO (no characteristic morphological changes, central distribution). Interstitial GGO refers to the uneven thickening of the alveolar wall caused by interstitial lymphatic reflux disorder. b. Atelectasis: it can be divided into obstructive atelectasis caused by bronchial mucous embolism and compression atelectasis caused by pleural effusion; c. Lung consolidation: Lung consolidation with the lobar and non-lobar distribution. ② Interstitial changes of the lungs: peripheral pulmonary interstitial changes, such as thickening of the interlobular septum and thickening of intralobular interstitium, and central pulmonary interstitial changes, such as thickening of bronchovascular bundle. ③ Lung nodules: soft tissue density, round or round-like, smooth margin, diameter 5–10 mm. ④ Airway abnormalities: thickening of the airway wall, airway stenosis, airway dilation. ⑤ Intrapulmonary signs: a. Tree-in-bud pattern: the 3–5 mm nodules and adjacent bronchioli formed this sign. The nodules were clustered and centrilobular adjacent to the bronchovascular bundle. b. Frog-spawn sign: Small nodules diffusely distributed in the lungs with reduced transparency. This sign resembles a frog-spawn in jelly-like mucus. c. Crazy-paving pattern: thickening of interlobular septa and/or intralobular interstitial within ground glass opacity.

MRL: (i) Abnormal lymphatic reflux: abnormal hyperintense on heavy T2-weighted imaging. (ii) Abnormal morphology of lymphatic vessels: spot-like or tubular, cystic intense on heavy T2-weighted imaging.

Statistical analysis

Statistical analysis was performed by using software (SPSS, version 26.0; IBM, Armonk, NY, USA). The Mcnemar paired chi-square test was used to compare the signs of abnormal lymphatic dilatation and reflux between CTL and MRL.*P*values less than 0.05 were considered to indicate statistical significance. The kappa test was used to evaluate the consistency of CTL and MRL in observing lymphatic abnormalities in patients with lymphatic PB. Kappa values were rated as follows: minor, less than 0.20; fair, 0.21 ~ 0.40; moderate, 0.41 ~ 0.60; good, 0.61 ~ 0.80; and almost perfect agreement, 0.81 ~ 1.00.

Results

Comparative analysis of MRL and CTL for abnormal lymphatic reflux

MRL was superior to CTL in detecting abnormal lymphatic reflux in the right lymphatic vessel, thoracic duct, cervical trunk and subclavian trunk ($P< 0.05$), with Kappa values of 0.205, 0.314, 0.367 and 0.387, respectively. The diagnostic consistency was fair. There was no significant difference in abnormal lymphatic reflux of the bronchial mediastinal trunk between the two groups ($P> 0.05$). The Kappa value was 0.640, and the diagnostic consistency was good (Table 1 and Fig. 2).

Comparative analysis of MRL and CTL for abnormal morphology of lymphatic vessels

MRL was better than CTL in detecting lymphatic abnormalities such as cystic changes at the extremity of the thoracic duct, spot-like or tubular changes at the

Table 1 Comparative Analysis of MRL and CTL for Abnormal Lymphatic Reflux

Lymphatic Reflux	Examinations		*Kappa* Value	*P* Value
	MRL	CTL		
Right lymphatic duct	25/31 (80.6)	10/31 (32.3)	0.205	0.001
Thoracic duct	26/31 (83.9)	19/31 (61.3)	0.314	0.039
Bronchial mediastinal trunk	26/31 (83.9)	22/31 (71.0)	0.640	0.125
Cervical trunk	10/31 (32.3)	3/31 (9.7)	0.367	0.016
Subclavian trunk	14/31 (45.2)	7/31 (22.6)	0.387	0.039

extremity of the right lymphatic duct, cystic changes at the extremity of the right lymphatic duct, and cystic changes in the mediastinum ($P<0.05$). The Kappa values were 0.175, 0.335, 0.205 and 0.415, respectively. The diagnostic consistency was minor, fair, fair and moderate, respectively. The two examinations showed no significant difference in showing mediastinal diffuse lymphatic abnormalities ($P>0.05$). The Kappa value was 0.912. The diagnostic consistency was almost perfect. There was no significant difference between the two groups ($P>0.05$) in showing spot-like or tubular changes in the subclavian region, cystic changes in the subclavian region, spot-like or tubular changes in the terminal of the thoracic duct, spot-like or tubular changes in the axilla, cystic changes in the axilla, spot-like or tubular changes in the mediastinum. The Kappa values were 0.459, 0.528, 0.470, 0.053, 0.367 and 0.433, respectively. The diagnostic consistency was minor, fair or moderate (Table 2 and Fig. 3).

Comparative analysis of MRL and CTL for lung abnormal signs

CTL was superior to MRL in detecting the thickening of the interlobular septum, lung nodules and airway stenosis ($P<0.05$). The Kappa values were 0.492, 0.424 and 0.197, respectively. The diagnostic consistency was moderate, moderate and minor. There was no significant difference between CTL and MRL detecting obstructive atelectasis, compression atelectasis, lobar and segmental consolidation, non-lobar and segmental consolidation, and thickening of bronchovascular bundle ($P>0.05$). The Kappa

Table 2 Comparative analysis of MRL and CTL for abnormal morphology of lymphatic vessels

Morphology	Examinations		*Kappa* Value	*P* Value
	MRL	CTL		
Subclavian region				
Spot-like or tubular	9/31 (29.0)	5/31 (16.1)	0.459	0.219
Cystic	5/31 (16.1)	2/31 (6.5)	0.528	0.250
The extremity of the thoracic duct				
Spot-like or tubular	18/31 (58.1)	18/31 (58.1)	0.470	1.000
Cystic	8/31 (25.8)	1/31 (3.2)	0.175	0.016
The extremity of the right lymphatic duct				
Spot-like or tubular	18 (58.1)	9/31 (29.0)	0.335	0.012
Cystic	7 (22.6)	1/31 (3.2)	0.205	0.031
Axilla				
Spot-like or tubular	6/31 (19.4)	4/31 (12.9)	0.053	0.727
Cystic	4/31 (12.9)	1/31 (3.2)	0.367	0.250
Mediastinum				
Diffuse	8/31 (25.8)	7/31 (22.6)	0.912	1.000
Limited				
Spot-like or tubular	23/31 (74.2)	22/31 (71.0)	0.433	1.000
Cystic	9/31 (29.0)	3/31 (9.7)	0.415	0.031

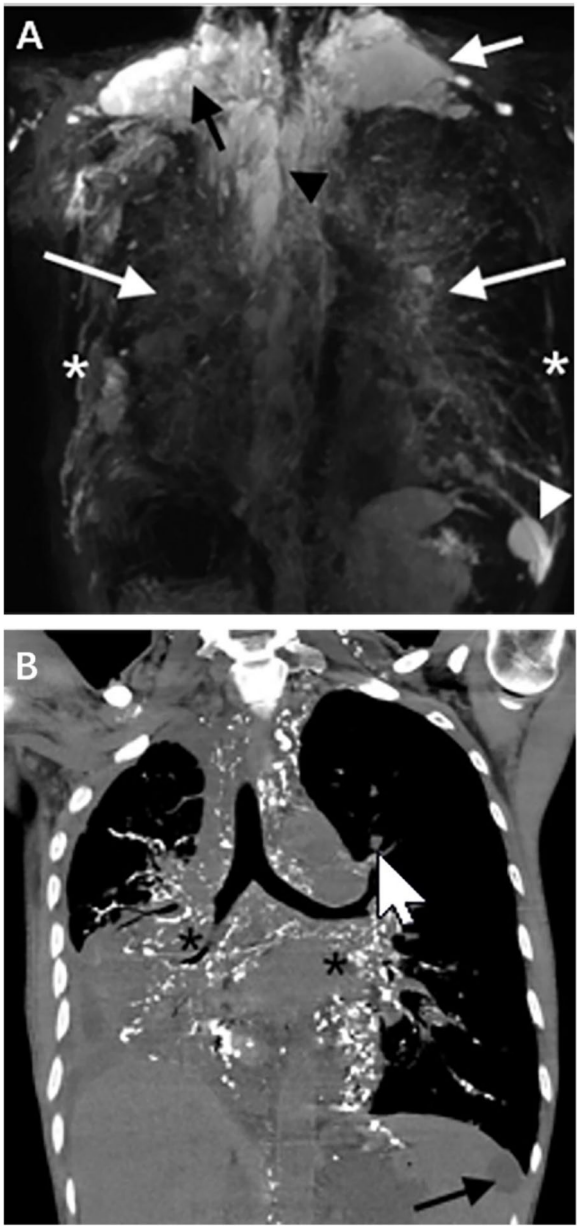

Fig. 3 **A** The coronal MRL shows multiple cystic hyperintense in the upper mediastinum *(black arrowhead)*, left neck *(white short arrow)*, right neck *(black short arrow)*, and spleen *(white arrowhead)*. Multiple tubular hyperintense were found in bilateral chest walls *(white asterisks)* and bilateral hilum *(white long arrows)*. **B** The coronal CTL shows abnormal contrast medium accumulation in the bilateral hilum *(black asterisk)*, and cystic hypodensity in the spleen *(black long arrow)*

values were 1.000, 0.912, 1.000, 0.652 and 0.746, respectively. A diagnostic agreement was almost perfect, almost perfect, almost perfect, good, and good. There was no significant difference between CTL and MRL in GGO, airway wall thickening and thickening of the intralobular interstitium ($P > 0.05$). Kappa values were 0.401, 0.384 and 0.135, respectively. The diagnostic agreement was fair, fair, and poor (Table 3 and Figs. 4, 5, 6 and 7).

Discussion

According to the literature [13–15], lymphatic PB is a disorder of lymphatic reflux caused by multiple etiologies. The pathogenesis may be increased lymph and coagulation after entering in the trachea to form a tree-like cast. Lymphatic PB is associated with primary lymphatic disease and postoperative congenital heart disease. The former is called primary lymphatic PB. This type is accompanied by primary lymphatic abnormalities [16]. The latter is referred to as secondary lymphatic PB. The specific clinical symptoms of lymphatic PB are coughing up or picking up bronchial tree-like substances with bronchoscopy. Other clinical symptoms are nonspecific, such as cough, sputum, chest tightness, and fever [17]. All 31 patients in this study were diagnosed with primary lymphatic PB because of a history of lymphatic dysplasia and the coughing up of tree-like casts. The clinical symptoms were consistent with the literature, mainly including fever, cough, chest tightness, chest pain, and hemoptysis [18, 19]. The treatment focuses on improving pulmonary ventilation function, including removing plastic substances under bronchoscopy [20], low-fat diet, aerosol, and embolization [21–23].

This study showed good agreement between MRL and CTL in showing abnormal lymphatic reflux in the bronchial mediastinal trunk. It may be that the bronchial mediastinal trunk has extensive drainage and collects lymph from most chest tissues, including the chest wall, pleura, mediastinum and lungs. It eventually converges

Table 3 Comparative analysis of MRL and CTL for lung abnormal signs

Abnormal Signs	Examinations		*Kappa* Value	*P* Value
	MRL	CTL		
Parenchymal changes of the lungs				
GGO	19/31 (61.3)	25/31 (80.6)	0.401	0.070
Parenchymal GGO	-	17/25 (68.0)	-	-
Acinar GGO	-	11/25 (44.0)	-	-
Ordinary GGO	-	6/25 (24.0)	-	-
Interstitial GGO	-	2/25 (8.0)	-	-
Mixed GGO	-	6/25 (24.0)	-	-
Atelectasis				
Obstructive atelectasis	1/31 (3.2)	1/31 (3.2)	1.000	1.000
Compression atelectasis	7/31 (22.6)	8/31 (25.8)	0.912	1.000
Consolidation				
Lobar and segmental distribution	1/31 (3.2)	1/31 (3.2)	1.000	1.000
Non-lobar and segmental distribution	1/31 (3.2)	2/31 (6.5)	0.652	1.000
Interstitial changes of the lungs				
Peripheral interstitial changes				
Interlobular septal thickening	8/31 (25.8)	16/31 (51.6)	0.492	0.008
Intralobular interstitial thickening	2/31 (6.5)	7/31 (22.6)	0.135	0.125
Central interstitial changes				
Bronchovascular bundles thickening	14/31 (45.2)	18/31 (58.1)	0.746	0.125
Pulmonary nodules	4/31 (12.9)	11/31 (35.5)	0.424	0.016
Airway abnormalities				
Airway wall thickening	24/31 (77.4)	26/31 (83.9)	0.384	0.687
Airway stenosis	2/31 (6.5)	12/31 (38.7)	0.197	0.002
Airway dilation	0/31 (0.0)	1/31 (3.2)	0.000	1.000
Other pulmonary signs				
Tree-in-bud pattern	-	3/31 (9.7)	-	-
Frog-spawn sign	-	3/31 (9.7)	-	-
Crazy-paving pattern	-	4/31 (12.9)	-	-

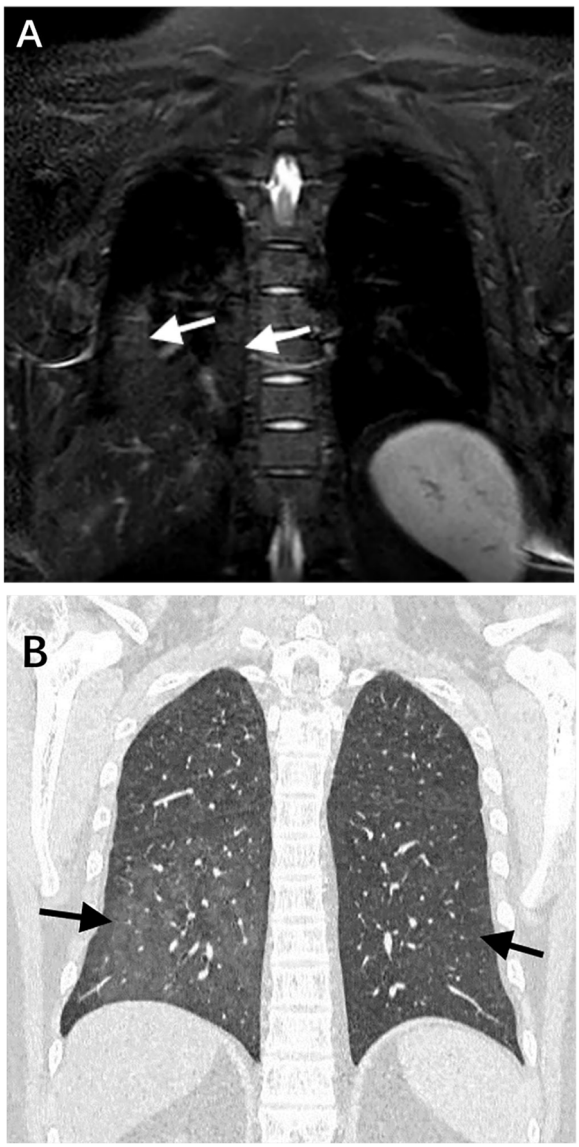

Fig. 4 **A** MRL shows hyperintense in the right lower lung *(white short arrow)*. **B** CTL shows increased transmittance of the lungs and diffuse distribution of GGO *(black short arrow)*

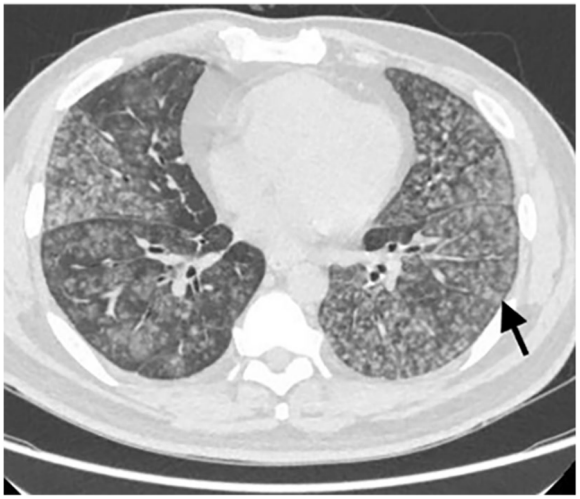

Fig. 5 The axial chest CT of lung window shows diffuse nodules in the lungs, with blurred edges and centered on acini *(black short arrow)*

Fig. 6 The chest CT of the lung window shows thickening of the right bronchovascular bundle *(black long arrow)* and ground glass opacity in the posterior segment of the right upper lobe *(asterisk)*

into the right lymphatic duct or thoracic duct [24, 25]. When the lymph of the bronchial mediastinal trunk is obstructed, extensive abnormal lymphatic proliferation can be seen. It shows abnormally hyperintense on heavy T2-weighted images on MRL and abnormal deposition of lipiodol on CTL. There were significant differences between MRL and CTL in showing abnormal lymphatic reflux in the right lymphatic duct, thoracic duct, cervical trunk and subclavian trunk. Besides, MRL has a higher detection rate. We speculate that MRL is more sensitive to displaying small lymphatic vessels and thus has a higher detection rate. When the lymphatic vessels are too small, or the lymph is less obstructed, the CTL was worse than MRL in detecting abnormal lymphatic reflux due to the slight pressure and the large volume of viscous lipiodol. In addition, the DLG of 2 patients showed that lipiodol stopped at the level of the first and second

lumbar vertebrae, respectively and did not continue to rise. It may be related to the heavier upstream obstruction. Therefore, no abnormal lipiodol deposition was observed in CTL.

Luo X et al. [26] have suggested that obstruction of the extremity of the thoracic duct may be one of the causes of abnormal lymphatic reflux in the chest. The patient's symptoms were relieved after the surgical release of the thoracic duct. In this study, 24 patients underwent thoracic duct outlet surgery and post-operative CT reexamination, and the CT signs of pulmonary lymphatic reflux disorder were alleviated or disappeared in 16 patients. The difference between MRL and CTL in this study was statistically significant in showing abnormal lymphatic reflux in the thoracic duct and right lymphatic duct. MRL detected more abnormalities than CTL. We classified the abnormal morphology of the lymphatic vessels as cystic and spot-like or tubular. The difference between these two examinations was statistically significant for cystic dilatation of the extremity of the thoracic duct and the extremity of the right lymphatic duct. We speculate that lipiodol into the dilated lymphatic vessels may affect the identification of its morphology. However, the observation by MRL is not affected by the contrast agent. Moreover, MRL has higher soft tissue resolution and better visualization of lymphatic vessels. In addition, the extremity of the thoracic duct and the extremity of the right lymphatic duct were most commonly spot-like or tubular dilatation. It is possible that the increased intraluminal pressure during obstruction makes compensatory dilation of the subclavian trunk, cervical trunk and bronchial mediastinal trunk, resulting in tubular structures at the extremity of the thoracic duct and right lymphatic duct. This study found that MRL could better display the morphological abnormalities of the thoracic duct and right lymphatic duct than CTL, which was consistent with literature [5, 9].

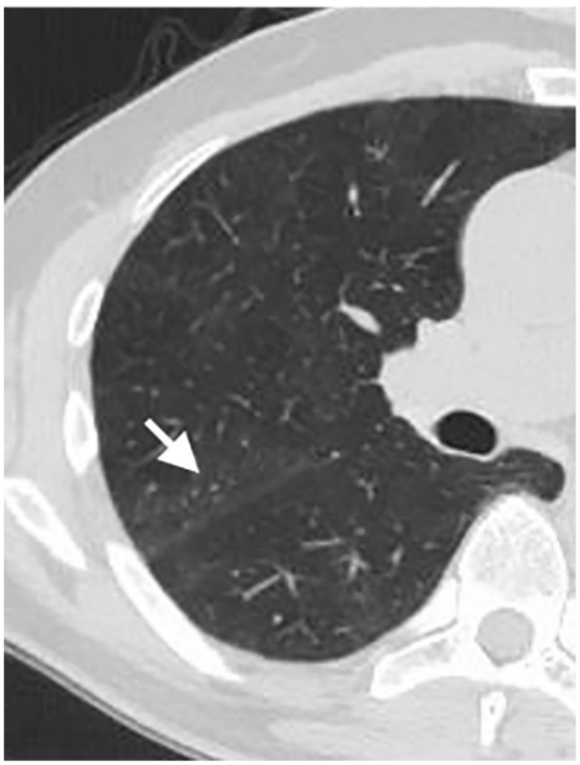

Fig. 7 The chest CT of the lung window shows multiple punctate nodules near the oblique fissure of the posterior segment of the right upper lobe, which was called "frog-spawn sign" *(white short arrow)*

O'Leary C [27] et al. studied 35 patients with lymphatic PB and found that GGO was more common in these patients than in non-lymphatic PB. Moreover, this sign can be a predictor of lymphatic PB. In our study, GGO was seen in 25 of 31 patients with lymphatic PB in CTL. 11 of these patients had a characteristic morphology and distribution of GGO in the form of clusters of alveolar GGO, which is called alveolar GGO. We hypothesized that the alveoli filling was caused by lymph aspiration into the acinar. GGO was observed in 19 patients with MRL. However, MRL could not distinguish the morphological features, and the diagnostic consistency was fair compared with CTL. In addition, the frog-spawn sign has not been reported in the literature and only can be seen in pulmonary lymphatic reflux disorders. We presumed that it was the dilated small lymphatic vessels in the lungs. In this study, CTL showed lung nodules in 11 patients, all of which were accompanied by the thickening of interlobular septum. We speculated that it was due to the abnormal proliferation of lymphatic vessels. MRL showed 4 patients with lung nodules, and the difference was statistically significant compared with CTL ($P<0.05$). The above signs have not been reported in the literature. The chest CTL and MRL of lymphatic PB patients also showed interstitial lung changes such as thickening of the interlobular septum, interlobular interstitium, bronchial vascular bundle, and parenchymal changes such as consolidation and atelectasis. The above signs are consistent with the literature [27]. In addition, MRL and CTL showed good or very good agreement in showing the thickening of the bronchovascular bundle, consolidation, and atelectasis. However, moderate or minor agreement shows the thickening of the interlobular septum and intralobular interstitium. We speculated that MRL was not as good as CTL in identifying the subtle signs. However, it was in good agreement with CTL in identifying the gross signs, such as atelectasis due to pleural effusion, extensive consolidation due to alveolar filling, or abnormal thickening of the bronchovascular bundle at the hilum.

There were some limitations to our study. Firstly, this was a retrospective study with small samples because of the rarity of this disease. Secondly, our study of lymphatic vessels lacked controls for the normal group. Thirdly, due to partial artifacts, the observation of partial thoracic ducts may be affected. Finally, all patients with primary lymphoblastic PB were included in this study, and no patients with secondary lymphoblastic PB were included. Whether the imaging findings of secondary lymphogenic PB are consistent with those of primary lymphogenic PB will be further explored in future studies.

In conclusion, lymphatic PB is a rare disorder of lymphatic reflux. MRL is superior to CTL in showing the abnormalities of lymphatic vessels. However, CTL was superior to MRL in the observation of abnormal signs in the lung. The combination of the two methods is valuable in diagnosing lymphatic PB.

Abbreviations

PB	Plastic bronchitis
MRL	Magnetic resonance lymphangiography
CTL	Computed tomography lymphangiography
CT	Computed tomography
DLG	Direct lymphangiography
GGO	Ground glass opacity

Clinical trial number

Not applicable.

Authors' contributions

(I) Conception and design: Qi Hao, Yan Zhang, Xiaoli Sun. (II) Administrative support: Rengui Wang, Nan Hong. (III) Provision of study materials or patients: Qi Hao, Yan Zhang, Xingpeng Li. (IV) Collection and assembly of data: Qi Hao, Yan Zhang, Xingpeng Li. (V) Data analysis and interpretation: Qi Hao, Yan Zhang, Xingpeng Li, Xiaoli Sun. (VI) Manuscript writing: All authors. (VII) Final approval of manuscript: All authors.

Funding

The work was supported by National Natural Science Foundation of China (grant no. 61876216 and 81971575).

Data availability

Data is provided within the manuscript.

Declarations

Ethics approval and consent to participate

The authors are accountable for all aspects of the work in ensuring that questions related to the accuracy or integrity of any part of the work are appropriately investigated and resolved. The study was conducted in accordance with the Declaration of Helsinki (as revised in 2013). The study was approved by the Ethics Committee of Beijing Shijitan Hospital, Capital Medical University, and informed consent was waived because the study was retrospective review.

Consent for publication

The images are entirely unidentifiable and there are no details on individuals reported within the manuscript.

Competing interests

The authors declare no competing interests.

Author details

[1]Department of Radiology, Peking University People's Hospital, No.11 Xizhimen South Street, Xicheng District, Beijing 100044, China. [2]Department of Radiology, Beijing Shijitan Hospital, Capital Medical University, Yangfangdian Tieyiyuan Road No.10, Haidian District, Beijing 100038, China. [3]Department of Radiology, Qilu Hospital of Shandong University, Jinan, China.

Received: 7 August 2024 Accepted: 18 November 2024
Published online: 23 December 2024

References

1. Rubin BK. Plastic bronchitis. Clin Chest Med. 2016;37(3):405–8.
2. Ntiamoah P, Mukhopadhyay S, Ghosh S, Mehta AC. Recycling plastic: diagnosis and management of plastic bronchitis among adults. Eur Respir Rev. 2021;30(161):210096.
3. Albitar HAH, Vassallo R. Lymphatic plastic bronchitis secondary to thoracic duct stenosis. Mayo Clin Proc. 2019;94(7):1141–2.
4. El Mouhadi S, Taillé C, Cazes A, Arrivé L. Plastic bronchitis related to idiopathic thoracic lymphangiectasia. Noncontrast magnetic resonance lymphography. Am J Respir Crit Care Med. 2015;192(5):632–3.
5. Cholet C, Delalandre C, Monnier-Cholley L, Le Pimpec-Barthes F, El Mouhadi S, Arrivé L. Nontraumatic chylothorax: nonenhanced mr lymphography. Radiographics. 2020;40(6):1554–73.
6. Cellina M, Martinenghi C, Panzeri M, Soresina M, Menozzi A, Daniele G, Oliva G. Noncontrast MR Lymphography in Secondary Lower Limb Lymphedema. J Magn Reson Imaging. 2021;53(2):458–66.
7. Cellina M, Gibelli D, Martinenghi C, Giardini D, Soresina M, Menozzi A, Oliva G, Carrafiello G. Non-contrast magnetic resonance lymphography (NCMRL) in cancer-related secondary lymphedema: acquisition technique and imaging findings. Radiol Med. 2021;126(11):1477–86.
8. Cè M, Menozzi A, Soresina M, Giardini D, Martinenghi C, Cellina M. Lymphedema Surgical Treatment Using BioBridgeTM: A Preliminary Experience. Appl Sci. 2023;13(20):11571.
9. Pabon-Ramos WM, Raman V, Schwartz FR, Tong BC, Koweek LM. Magnetic resonance lymphangiography of the central lymphatic system: technique and clinical applications. J Magn Reson Imaging. 2021;53(2):374–80.
10. Pan F, Loos M, Do TD, Richter GM, Kauczor HU, Hackert T, Sommer CM. The roles of iodized oil-based lymphangiography and post-lymphangiographic computed tomography for specific lymphatic intervention planning in patients with postoperative lymphatic fistula: a literature review and case series. CVIR Endovasc. 2020;3(1):79.
11. Jin D, Sun X, Shen W, Zhao Q, Wang R. Diagnosis of lymphangiomatosis: a study based on ct lymphangiography. Acad Radiol. 2020;27(2):219–26.
12. Patel S, Hur S, Khaddash T, Simpson S, Itkin M. Intranodal CT lymphangiography with water-soluble iodinated contrast medium for imaging of the central lymphatic system. Radiology. 2022;302(1):228–33.
13. Itkin MG, McCormack FX, Dori Y. Diagnosis and treatment of lymphatic plastic bronchitis in adults using advanced lymphatic imaging and percutaneous embolization. Ann Am Thorac Soc. 2016;13(10):1689–96.
14. Itkin M, Chidekel A, Ryan KA, Rabinowitz D. Abnormal pulmonary lymphatic flow in patients with paediatric pulmonary lymphatic disorders: diagnosis and treatment. Paediatr Respir Rev. 2020;36:15–24.
15. O'Leary CN, Khaddash T, Nadolski G, Itkin M. Abnormal pulmonary lymphatic flow on novel lymphangiographic imaging supports a common etiology of lymphatic plastic bronchitis and nontraumatic chylothorax. Lymphat Res Biol. 2022;20(2):153–9.
16. Ozeki M, Fujino A, Matsuoka K, Nosaka S, Kuroda T, Fukao T. Clinical features and prognosis of generalized lymphatic anomaly, kaposiform lymphangiomatosis, and gorham-stout disease. Pediatr Blood Cancer. 2016;63(5):832–8.
17. Tomasulo CE, Chen JM, Smith CL, Maeda K, Rome JJ, Dori Y. Lymphatic disorders and management in patients with congenital heart disease. Ann Thorac Surg. 2022;113(4):1101–11.
18. Mehta I, Patel K. Lymphatic plastic bronchitis. N Engl J Med. 2022;386(8):e19.
19. Siddiqi NH, Kraman SS, Pressman B. Adult-onset plastic bronchitis with novel lymphatic anatomy: cured with endo-lymphatic embolization. Respiration. 2019;98(2):171–3.

20. Soyer T, Yalcin Ş, Emiralioğlu N, Yilmaz EA, Soyer O, Orhan D, Doğru D, Sekerel BE, Tanyel FC. Use of serial rigid bronchoscopy in the treatment of plastic bronchitis in children. J Pediatr Surg. 2016;51(10):1640–3.
21. Sriram K, Meguid RA, Meguid MM. Nutritional support in adults with chyle leaks. Nutrition. 2016;32(2):281–6.
22. Robinson M, Smiley M, Kotha K, Udoji T. Plastic bronchitis treated with topical tissue-type plasminogen activator and cryotherapy. Clin Pediatr (Phila). 2016;55(12):1171–5.
23. Pieper CC, Hart C, Schneider M, Asfour B, Attenberger UI, Herberg U. Transabdominal lymphatic embolization during extracorporeal membrane oxygenation as an urgent treatment of cataclysmic, uncontrollable plastic bronchitis. J Vasc Interv Radiol. 2021;32(5):766–8.
24. Lee GM, Stowell JT, Pope K, Carter BW, Walker CM. Lymphatic pathways of the thorax: predictable patterns of spread. AJR Am J Roentgenol. 2021;216(3):649–58.
25. Sun JD, Shum T, Behzadi F, Hammer MM. Imaging findings of thoracic lymphatic abnormalities. Radiographics. 2022;42(5):1265–82.
26. Luo X, Zhang Z, Wang S, Gu X, Wang X. Chyloptysis with chylopericardium, a rare case and mini-review. BMC Pulm Med. 2018;18(1):21.
27. O'Leary C, Itkin M, Roshkovan L, Katz S, Cao Q, Hershman M, Galperin-Aizenberg M. CT features of lymphatic plastic bronchitis in adults: correlation with multimodality lymphatic imaging. Radiol Cardiothorac Imaging. 2022;4(2):e210048.

Publisher's Note